RSC Advances

ROYAL SOCIETY OF CHEMISTRY

www.rsc.org/advances

Graphical abstract

Food grade monodisperse O/W emulsions encapsulating ergocalciferol have been formulated using microchannel emulsification. The O/W emulsion droplets have encapsulation efficiency of over 85% within the evaluated storage period.

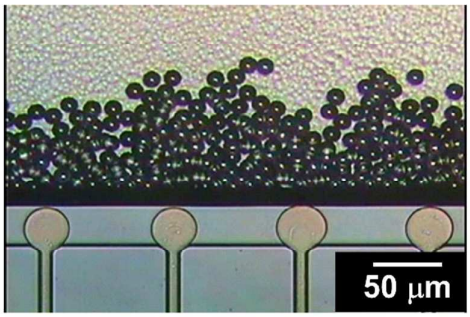

Typical droplet generation encapsulating ergocalciferol in grooved microchannel emulsification

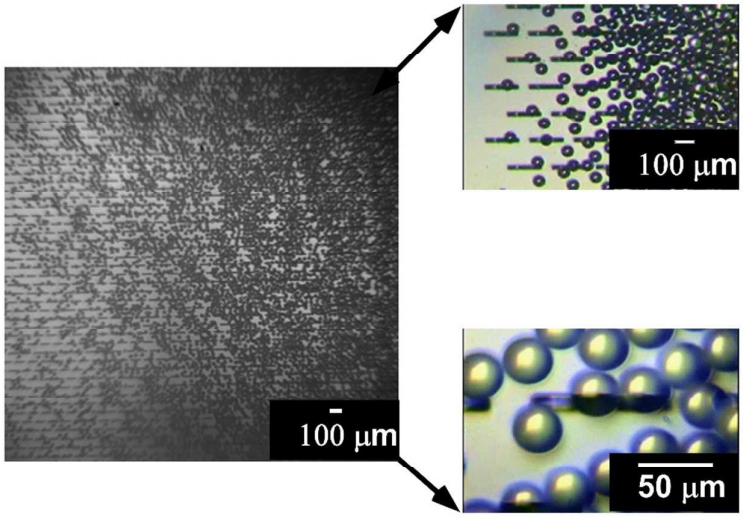

O/W emulsion encapsulating ergocalciferol in straight through microchannel emulsification

Formulation characteristics of triacylglycerol oil-in-water emulsions loaded with ergocalciferol using microchannel emulsification

Nauman Khalid[a, b, c], Isao Kobayashi[a,*], Zheng Wang[a, c], Marcos A. Neves[a, c], Kunihiko Uemura[a], Mitsutoshi Nakajima[a, c] and Hiroshi Nabetani[a, b]

[a] Food Engineering Division, National Food Research Institute, NARO, 2-1-12 Kannondai, Tsukuba, Ibaraki 305-8642, Japan

[b] Graduate School of Agricultural and Life Sciences, The University of Tokyo, 1-1-1 Yayoi, Bunkyo-ku, Tokyo 113-8657, Japan

[c] Faculty of Life and Environmental Sciences, University of Tsukuba, 1-1-1 Tennoudai, Tsukuba, Ibaraki 305-8572, Japan

* Corresponding Author. Tel.: 81 29 838 8025; fax: +81-29-838-8122.

E-mail address: isaok@affrc.go.jp (I. Kobayashi)

Ergocalciferol is one the important form of vitamin D that is needed for proper functioning of human metabolic system. The study formulates monodisperse food grade ergocalciferol loaded oil-in-water (O/W) emulsions by microchannel emulsification (MCE). The primary characterization was performed with grooved MCE, while storage stability and encapsulating efficiency (EE) was investigated with straight-through MCE. The grooved microchannel (MC) array plate has 5×18-μm MCs, while asymmetric straight-through MC array plate consists of numerous 10×80-μm microslots each connected to a 10 μm-diameter circular MC. Ergocalciferol at a concentration of 0.2-1.0% (w/w) was added to various oils and served as the dispersed phase, while the continuous phase constituted either of 1% (w/w) Tween 20, decaglycerol monolaurate (Sunsoft A-12) or β-lactoglobulin. The primary characterization indicated successful emulsification in the presence of 1% (w/w) Tween 20 or Sunsoft A-12. The average droplet diameter increased slowly with increasing concentration of ergocalciferol and ranged from 28.3 to 30.0 μm with coefficient of variation below 6.0%. Straight-through MCE was conducted with 0.5% (w/w) ergocalciferol in soybean oil together with 1% (w/w) Tween 20 in Milli-Q water as optimum dispersed and continuous phases. Monodisperse O/W emulsions with Sauter mean diameter ($d_{3,2}$) of 34 μm with relative span factor of less than 0.2 were successfully obtained from straight-through MCE. The resultant oil droplets were physically stable for 15 d at 4 ^{o}C without any significant increase in $d_{3,2}$. The monodisperse O/W emulsions exhibited ergocalciferol EE of more than 75% during the storage period.

Keywords: Microchannel emulsification, Asymmetric microchannel, Grooved microchannel, Oil-in-water emulsions, Monodisperse droplets, Ergocalciferol, Emulsifier concentration, Droplet generation, Dispersed phase flux

Introduction

Vitamin D plays a vital role in maintaining and developing healthy human skeletal system, since it maintains calcium level in the body. Deficiency of vitamin D results in increased risk of diabetes, hypertension, cancer and autoimmune diseases.[1-4] Broad spectrum deficiencies of vitamin D include rickets in children, osteomalacia in adults and osteoporosis in women, all of these lead to softening and weakening of bones.[5-7] Nutritional and cultural factors leading to vitamin D deficiency include insufficient fortified food consumption, sun-block usage, limited body exposure to sun and fear for excessive intake of vitamin D.[7,8] Vitamin D is synthesized in the skin and involves the phytochemical conversion of pro-vitamin D by the action of ultraviolet (UV-B) rays. This process takes place if the UV-B rays fall between 290-315 nm of spectrum. These rays are only emitted in the regions that lie below 35^{o} latitude.[9,10]

The terminology and classification related to vitamin D is confusing and can be classified into 5 different forms and metabolites. Among these vitamin D_2 (ergocalciferol) and D_3 (cholecalciferol) are important (Fig. 1).[11,12] Vitamin D_2 is naturally present in some plants and is produced commercially by UV irradiation of yeast, while vitamin D_3 is naturally produced in human and animal bodies. Vitamin D_2 is substantially used for fortification and supplementation in food and pharmaceutical industries. [12] Several researchers pointed out rapid metabolism of vitamin D_2 in comparison to vitamin D_3, while the action become bioequivalent if taken daily.[13,14] Both forms of vitamin D are converted to 25-hydoxy vitamin D [25-(OH)D] in the liver. The quantification of 25-(OH)D in blood gives the quantitation of vitamin D status. A cutoff value of 30 ng mL^{-1} is sometimes used for optimal vitamin D status.[12] Ergocalciferol was produced in 1920s through UV-B exposure of foods, leading to the formation of first medicinal preparation called Viosterol.[15] Ergocalciferol has limited natural sources and the most significant source is wild mushrooms.[16] Ergocalciferol is prone to oxidation and is also isomerized to isotachysterol in the presence of

sunlight and mostly under acidic conditions.[16,17] Ergocalciferol is mostly supplemented and fortified in fat based products due to its hydrophobic nature.

Emulsification technologies play an important role in the production of encapsulated foods, pharmaceuticals, cosmetics and chemicals.[18,19] The emulsions are usually either single (O/W and W/O) emulsions or double emulsions (W/O/W and O/W/O).[19] These different emulsion systems are produced by either conventional devices including colloid mills, high pressure homogenizers and rotor-stator homogenizers or modern devices such as microfluidic devices (lab-on-a-chip), membrane emulsification and microchannel emulsification (MCE) devices.[19,20] Conventional devices produce polydisperse emulsions with broader size distributions, which in turn reduce the emulsion stability and functionality. Microfabricated emulsification devices have potential to produce monodisperse emulsions with the smallest coefficient of variation (CV) less than 10% for membrane emulsification and around 5% for microfluidic devices and MCE.[20]

MCE is a progressive technique that enables production of monodisperse emulsions by spontaneous transformation of oil-water interface specifically driven by interfacial tension dominant on a micron scale.[21] MCE studies were comprehensively reviewed by Vladisavljević *et al*.[20,22] Similarly, this emulsification technique allows integration of hundreds of thousands of droplet generation units on a single plate.[23,24] MCE has been used for producing O/W, W/O and W/O/W emulsions with diameters ranged from 1 μm to 550 μm.[22] Based on microfabrication design, the MCE devices can either be categorized into grooved microchannel (MC) arrays each consisting of uniform microgrooves and a slit-like terrace and straight-through MC arrays each having uniform asymmetric microholes together with microslots.[22] Grooved MC array plates are further classified into dead-end and cross-flow types. Grooved MCE plates of cross-flow type are particularly useful to observe the entire droplet generation process together with droplet collection at low dispersed phase flow rates.[25,26] On the other hand, straight-through MC arrays are designed to improve the throughput

capacity of MCE. Straight-through MC arrays have ability to increase the production capacity of monodisperse emulsion droplets over 2000 L m^{-2} h^{-1}.[22]

MCE has also been used to produce monodisperse microdispersions (e.g. solid lipid microspheres[26], gel microbeads[27], and giant vesicles[28]). MCE has promising potential for producing uniformly sized oil droplets containing functional lipids such as β-carotene[29], γ-oryzanol[30], L-ascorbic acid[31], ascorbic acid derivatives[32], oleuropein[33], and vitamin D.[34] Different food grade materials (e.g. refined vegetable oils, a medium-chain triglyceride oil, hydrophobic and hydrophilic emulsifiers, proteins, and hydrocolloids) were utilized to produce monodisperse O/W, W/O, W/O/W emulsions and microparticles by MCE. [35,36]

We previously encapsulated vitamin D (both vitamin D_2 and D_3) in O/W emulsions using MCE and reported long-term stability studies and encapsulation efficiencies of O/W emulsions encapsulating vitamin D_2 and D_3.[34] Ergocalciferol is a plant-based vitamin D type, and previous studies seldom report its encapsulation in different formulations. Keeping its rapid metabolism rate and importance in human diet, the present study was conducted to encapsulate only ergocalciferol in triacylglycerol oil-in-water emulsions using MCE. The basic characterization and optimization of these emulsions were performed using a grooved MC array plate. Straight-through MCE was carried out to investigate the effect of dispersed phase flux on the production characteristics and as well as physical and chemical stability of ergocalciferol-loaded O/W emulsions. The effects of different triacylglycerol oils and emulsifiers on preparation characteristics of O/W emulsions by MCE were also evaluated. The results of this research are expected to formulate new aqueous based functional foods.

Experimental

Chemicals

Ergocalciferol, polyoxyethylene (20) sorbitan monolaurate (Tween 20), olive oil, and soybean oil were purchased from Wako Pure Chemical Industries Ltd. (Osaka, Japan). Medium chain triacylglycerol (MCT, sunsoft MCT-7) with a fatty acid residue composition of 75% caprylic acid and 25% capric acid and decaglycerol monolaurate (Sunsoft A-12) were procured from Taiyo Kagaku Co. Ltd. (Yokkaichi, Japan). Safflower oil was purchased from MP biomedicals (lllkirch, France). β-Lactoglobulin (β-lg) from bovine milk (>90% purity) was purchased from Sigma-Aldrich Co. LLC. (St. Louis, USA). All other chemicals used in this study were of analytical grade and used as received.

Preparation of solutions

The continuous phase was prepared by dissolving either 1% (w/w) Tween 20, 1% (w/w) Sunsoft A-12 or 1% (w/w) β-lg in Milli-Q water with a resistivity of 18MΩ cm. The dispersed phase was prepared by dissolving 0.2-1.0% (w/w) ergocalciferol in MCT, soybean, olive or safflower oil at 85 ^{o}C ± 3 ^{o}C for 20 min and afterwards cooling at room temperature for 2 h before storage at 4 ± 1 ^{o}C. During storage, dissolved ergocalciferol molecules could form nuclei whose growth eventually makes crystals large enough to sediment. Before initiating experiments, the samples were therefore shaken slightly to avoid formation of any ergocalciferol crystals.

Silicon plates for MCE

The experiments have been carried out by using silicon MC array plates (model CMS 6-2 and WMS11-1, EP. Tech Co., Ltd., Hitachi, Japan). Fig. 2a is a schematic representation of a CMS 6-2 plate with 540 parallel channels on 10 consecutive MC arrays. Each MC array contains 54 parallel MCs with a depth of 5 μm, a width of 18 μm and a length of 140 μm and a terrace with a depth of 5 μm and a length of 60 μm. Each continuous-phase channel outside the terrace outlet has a depth of 100 μm. Fig. 2b is a schematic representation of a WMS 11-1 plate with 27,400 MCs compactly arranged within a 10 × 10 mm square region in the plate center. Each MC consists of a cylindrical 10

μm diameter straight microhole with a depth of 200 μm and a 10 × 80 μm microslot with a depth of 40 μm. The slot aspect ratio of 8 was above the threshold value of 3 for successfully generating monodisperse emulsion droplets.[37] The distance between the two adjacent MCs in the vertical was 105 μm, and the distance between the centers of MCs in the adjacent rows was 70 μm. The MC array plates were subjected to plasma oxidation in plasma reactor (PR41, Yamato Science Co. Ltd., Tokyo, Japan) to activate a silicon dioxide layer on their surfaces. The activated silicon dioxide layer is capable of maintaining their hydrophilicity during MCE.

Experimental procedure for MCE

For grooved MCE, the setup consists of an MC module, a 10 mL liquid chamber that contains the disperse phase and a syringe pump (Model 11, Harvard Apparatus Inc., Holliston, USA) that feeds the continuous phase with a 50 mL glass syringe (Fig. 3a). MCE was carried out for approximately 3 h and monitored through an inverted metallographic microscope equipped with an objective lens of 2.5x to 20x and a CCD camera (MS-511B, Seiwa Kougaku Sesakusho Ltd., Tokyo, Japan). The whole process was recorded with a video recorder (RDR-HX67; Sony Co., Tokyo, Japan). Droplet-generation experiments were performed with the grooved MCE setup depicted in Fig. 3b. The module was initially filled with the continuous phase before mounting the CMS 6-2 plate. The pressurized dispersed phase was introduced into the module. The pressure applied to the dispersed phase (ΔP_d) was gradually increased. ΔP_d can be given by

$$\Delta P_d = \rho_d \Delta h_d g \qquad (1)$$

where ρ_d is the dispersed-phase density, Δh_d is the difference in the hydraulic heads between the chamber containing the dispersed phase and the channels of the module, and g is the acceleration due to gravity. To generate droplets, the dispersed phase was forced through the MCs onto the terrace and into the continuous phase channel.

For straight-through MCE, the MC array plate was degassed in a continuous aqueous phase by ultrasonic bath for 20 min and the setup consists of an MC module (comprising of six steel parts and two glass plates of different dimensions and rubber seals) and syringe pumps (Model 11, Harvard Apparatus Inc.) that feed the continuous and dispersed phases (Fig. 4a). MCE was carried out for approximately 1 h and monitored through FASTCAM-1024 PCI high speed video system at 250 to 500 fps (Photron Ltd., Tokyo, Japan) attached to the inverted metallographic microscope. The droplet generation process was depicted in Fig. 4b. Droplet generation started with injecting the disperse phase through the syringe pump at the dispersed phase flow rate (Q_d) ranging from 0.5 to 2.0 mL h^{-1} (5 to 20 L m^{-2} h^{-1} in dispersed phase flux (J_d)). The generated droplets were removed by varying the continuous phase flow rate (Q_c) from 100 to 500 mL h^{-1} through the gap between the MC array plate and the glass plate. The shear stress (τ) in the module surrounding the WMS 11-1 plate is given by

$$\tau = \frac{3Q_c n_c}{2h^2 W} \qquad (2)$$

where h =1 mm is the gap height and W = 12 mm is the gap width, and η_c is the continuous phase viscosity. τ had a negligible value of 0.002 to 0.02 Pa at the Q_c range applied in this study. After each experiment the MC array plates were cleaned in three steps. In the first step the MC array plates were washed with neutral detergent together with Milli-Q water in an ultrasonic bath (VS-100 III, As One Co., Osaka, Japan) for 20 min, afterwards treatment with 50% Milli-Q water and 50% ethanol in an ultrasonic bath, lastly cleaned in an ultrasonic bath with Milli-Q water and stored in 50 mL of Milli-Q water prior to reuse for MCE.

Determination of droplet size and droplet size distribution

The size and size distribution of the resultant O/W emulsion droplets from grooved MCE were determined as follows. The average droplet diameter (d_{av}) was defined by

$$d_{av} = \sum_{i=1}^{n} d_i / n \qquad (3)$$

where d_i is the diameter of the i^{th} droplet measured using WinRoof software (Mitani Co., Ltd., Fukui, Japan) and n is the number of the droplets measured (n= 250). The droplet size distribution was expressed as CV, and is defined as

$$\mathrm{CV} = \frac{\sigma}{d_{av}} \times 100 \qquad (4)$$

where σ is the standard deviation and d_{av} is the average droplet diameter.

The droplet size distribution of the O/W emulsions obtained from straight-through MCE was measured by using a laser scattering instrument that works on the principle of Polarization Intensity Differential Scattering Technology (LS 13 320, Beckman Coulter, Inc., Brea, USA). This instrument have ability to measure the size ranging from 0.04 to 2000 μm with a resolution of 116 particle size channels. The mean droplet size was expressed as Sauter mean diameter ($d_{3,2}$), defined as the diameter of a droplet having the same area per unit volume as that of the total collection of droplets in emulsions. The width of droplet size distribution was expressed as relative span factor (RSF), defined as

$$\mathrm{RSF} = \frac{d_{v0.9} - d_{v0.1}}{d_{v0.5}} \qquad (4)$$

where $d_{v0.9}$ and $d_{v0.1}$ are the representative diameters where 90% and 10% of the total volume of the liquid is made up of droplets with diameters smaller than or equal to the stated value, and $d_{v0.5}$ is the representative diameter where 50% of the total volume of the liquid is made up of droplets with diameters larger than the stated value and 50% is made up of droplets with diameters smaller than the stated value.

Measurement of fluid properties

206 The densities of dispersed and continuous phases were measured using a density meter (DA-130 N,
207 Kyoto Electronics Manufacturing Co., Ltd., Kyoto, Japan) at 25 ± 2°C. Their viscosities were
208 measured with a vibro viscometer (SV-10, A&D Co., Ltd., Tokyo, Japan) at 25 ± 2°C by taking
209 either 10 or 35 mL of samples in a measuring vessel followed by immersion of sensor plates in that
210 vessel. Viscosity was measured by detecting the electric current needed to resonate the sensor plates.
211 The static interfacial tension between the preceding two phases was measured with a fully automatic
212 interfacial tensiometer (PD-W, Kyowa Interface Sciences Co., Ltd., Saitama, Japan) using a pendant
213 drop method. The key physical properties of the dispersed and continuous phases used in this study
214 are presented in Table 1.

215 **Physical and chemical stability of O/W emulsions**

216 The physical stability of the O/W emulsion droplets loaded with ergocalciferol was evaluated
217 according to the method described in an earlier section. The $d_{3,2}$, RSF, consistency and coalescence
218 during 15 d of storage at 4±1 °C under dark conditions were observed.

219 The amount of ergocalciferol encapsulated in the O/W emulsions was determined
220 spectrophotometrically. All spectral measurements of the ethanolic extracts of these O/W emulsions
221 were carried out using a UV/VIS/NIR spectrophotometer (UV-1700, Shimadzu Co., Kyoto, Japan).
222 First, 1 mL of the emulsion was mixed with 9 mL of ethanol, followed by ultrasonication for 20 min.
223 The ethanolic extracts were then centrifuged (Avanti HP-25, Beckman Coulter, Inc.) at 20,000 *g* for
224 15 min. A 1 mL aliquot of the subnatants was diluted ten times with ethanol and then injected into a
225 quartz cell with a 10 mm pass length. The absorbance of ergocalciferol in emulsion extract was
226 measured at 310 nm using an appropriate blank. A representative standard curve of absorbance
227 versus concentration gave linear least-squares regression with a coefficient of determination (r^2) of
228 0.9996. All experiments were repeated in triplicate and mean values were calculated. The Beer's law
229 was obeyed in the concentration range of 0.1-0.5 mg mL^{-1} and the sensitivity of measurement has

relative standard deviation of 0.85% (n=15). The Molar absorptivity ($\mathcal{E}$) for ergocalciferol during this study was 2.52 mM^{-1} cm^{-1}. The encapsulation efficiency (EE) of ergocalciferol in samples were calculated with the equation

$$EE = \frac{W_t}{W_0} \times 100 \qquad (5)$$

where W_t is the total amount of ergocalciferol in the O/W emulsions at a specific time (t) and W_o is the total amount of ergocalciferol initially quantified at day 1.

Results and discussion

Basic droplet generation characteristics through grooved MCE

Effect of disperse phase composition

Fig. 5a illustrates the effect of different oils on the d_{av} and CV of the O/W emulsions prepared using CMS6-2 plate. MCE was carried out using 0.5% (w/w) ergocalciferol in MCT, soybean, olive or safflower oil as the dispersed phase and 1% (w/w) Tween 20 in Milli-Q water as the continuous phase. A gradual increase in ΔP_d caused the dispersed phase to enter the terrace in front of the MC inlets. When ΔP_d reached the break-through pressure of about 3.0 kPa, the dispersed phase started to pass through the MCs, leading to the periodic generation of oil droplets. The MCE was performed at a ΔP_d of 3.2 kPa slightly higher than the break-through pressure. Q_c was fixed at 2 mL h^{-1} throughout the experiment. Successful generation of monodisperse O/W emulsion droplets took place, regardless of the oil types used. The d_{av} of the resultant O/W emulsions loaded with ergocalciferol ranged from 28.3 to 30.0 μm with CV between 3.6 and 6.1%. Fig. 5b(*i-iv*) shows the droplet detachment process with different dispersed phases. The different dispersed phase solutions exhibited successful emulsification with smooth detachment of droplets from the terrace outlets, and narrower droplet size distributions were seen in the emulsions prepared with olive oil, safflower oil and soybean oil in comparison to MCT (Fig. 5c). The O/W emulsions prepared with MCT had a

somewhat greater CV of about 6%. Uniformly sized droplets are stably generated in MCE, if the inflow of the continuous phase toward the terrace is sufficiently fast compared to the outflow of the dispersed phase from the MC outlets.[38] The viscosity ratio ($\zeta = \eta_d/\eta_c$) is also a key factor determining the monodispersity of emulsions.[38] The viscosity ratio of all the oils used in this study was sufficiently high (Table 1), leading to successful preparation of monodisperse O/W emulsions encapsulating ergocalciferol. The less monodispersity with MCT might be attributed to some attractive interaction of MCT with MC and terrace surfaces. Such interaction causes slight increase in CV of O/W emulsion droplets in comparison to other viscous oils. Tan *et al.* [39] pointed out that hydrophobicity of the dispersed phase is the critical parameter affecting the generation of oil droplets in MCE.

Effect of different emulsifiers

The effect of the emulsifier type on oil droplet generation by grooved MCE was also investigated. Food-grade hydrophilic emulsifiers (Tween 20, Sunsoft A-12 and β-lg) with a noticeable ability to prepare O/W emulsions were used at a concentration of 1% (w/w) in the Milli-Q water. These aqueous emulsifier solutions were used as the continuous phase. 0.5% (w/w) ergocalciferol in soybean oil was used as the dispersed phase. The important physical properties of different emulsifiers were presented in Table 1. There was not a prominent difference in the viscosity and density values of emulsifier solutions, while β-lg had higher interfacial tension (12.6 mN m^{-1}) in comparison to Tween 20 and Sunsoft A-12. All of these emulsifier solutions exhibited successful emulsification with smooth detachment of droplets from the terrace outlets (Fig. 6a). Uniformly-sized emulsion droplets were stably generated from the MCs especially in the presence of Tween 20 and Sunsoft A-12. There was neither the generation of bigger droplets nor a continuous outflow of dispersed phase. Fig. 6b illustrates the effect of the emulsifier type on the d_{av} and CV of O/W emulsions. The d_{av} and CV of the resultant O/W emulsions were 28.5 μm and 5.9% for Tween 20 and 28.1 μm and 6.6% for Sunsoft A-12. Uniformly-sized droplets stabilized by Tween 20 or

Sunsoft A-12 were successfully generated due to high interfacial activity, as these emulsifiers have low interfacial tension values of about 5.0 mN m^{-1}. Droplet generation and detachment processes for β-lg at pH 7.3 were initially stable with the smallest d_{av} of 26.6 μm. However, after 5 min few droplets started sticking in the well (Fig. 6a(*iii*) and Fig. 6c) and coalesced with passage of time, resulting in the increase of CV value to 7.2%. The result suggests that β-lg did not adsorb strongly at the newly created interface, presumably because the weak electrostatic interactions between ergocalciferol and β-lg clearly observed from high interfacial tension value.

Kobayashi and Nakajima[40] investigated the effect of the emulsifier type on droplet generation characteristics by using a straight-through extrusion filter. They reported Tween 20 and decaglyerol monolaurate as suitable, hydrophilic food-grade emulsifiers in MCE without ergocalciferol. Patel and San Martin-Gonzalez[17] also demonstrated successful preparation of solid lipid nanoparticles loaded with ergocalciferol stabilized by Tween 20. The preceding results demonstrate that Tween 20 and Sunsoft A-12 as potential emulsifiers for generating ergocalciferol-loaded O/W emulsions, either with conventional homogenization techniques (data not shown) or MCE.

Effect of ergocalciferol concentration

Fig. 7 illustrates the effect of concentration of ergocalciferol on the d_{av} and CV of the O/W emulsions prepared using two different emulsifiers and CMS6-2 plate. The concentration of ergocalciferol varied from 0.2% to 1.0% (w/w) in soybean oil. According to US Pharmacopeia, ergocalciferol is sparingly soluble in different oils but have good solubility in organic solvents, except hexane. In our study, we noticed a maximum solubility of 1% (w/w) ergocalciferol in different oils at 85 ± 2°C with no solubility at room temperature. Successful MCE was conducted with different concentrations of ergocalciferol by keeping ΔP_d at 3.2 kPa and Q_c around 2 mL h^{-1}. The d_{av} of the ergocalciferol-loaded O/W emulsions increased slowly with increasing concentration of ergocalciferol when emulsified with 1% (w/w) Tween 20. Their d_{av} ranged between 23.8 and 28.5

μm with CV between 5.9 and 6.2%. Comparatively similar results were obtained with Sunsoft A-12 (Fig. 7). The ergocalciferol-loaded O/W emulsions stabilized with 1% (w/w) Sunsoft A-12 had d_{av} of 24.5 to 27.5 μm and have CV of 6.5 to 8.4%. A better droplet size distribution expressed as a smaller CV was seen in the emulsions stabilized with Tween 20 in comparison to those stabilized with Sunsoft A-12 (Fig. 7). A reason behind the increased d_{av} with increasing ergocalciferol concentration could be attributed to weak attractive interaction between oil encapsulating ergocalciferol and MC and terrace surfaces during MCE. These types of interactions with terrace surfaces in MCE during L-ascorbic acid encapsulation were previously reported by Khalid *et al*.[41] To remain in optimum range and easiness of the process we conducted stability and encapsulating efficiency experiments by using 0.5% (w/w) ergocalciferol in soybean oil as an optimum dispersed phase. Moreover, this concentration has no effect on different parameters, since we evaluated low and high concentration effect also. The other reason for choosing this concentration is to make process more practical at industrial scale; i.e., 0.5% (w/w) ergocalciferol in the dispersed phase is mostly desired in different industries.

Effect of dispersed phase flow rate

Dispersed phase flow rate (Q_d) is an important parameter in MCE that correlates with droplet productivity at the stable droplet generation regime. Fig. 8a depicts the effect of Q_d on the d_{av} and CV of the droplets generated using CMS6-2 plate. The dispersed phase constitutes 0.5% (w/w) ergocalciferol in soybean oil, while the continuous phase includes 1% (w/w) Tween 20 in Milli-Q water.

At the lowest Q_d of 2×10^{-3} mL h^{-1}, the resultant droplets with a monomodal and very narrow size distribution had a d_{av} of 23.5 μm and a CV of 5.4%. When Q_d was increased stepwise, monodisperse emulsions with CV of 4 to 10% were produced at Q_d of 8×10^{-2} mL h^{-1} or less. In this Q_d range, d_{av} of the resultant droplets ranged from 23.7 μm to 26.7 μm. The microscopic

observations during MCE confirmed that the resultant droplet size hardly changed at Q_c between 0 mL h^{-1} and 5.0 mL h^{-1}. The generation of droplets even without external flow of the continuous phase depicts the unique spontaneous transformation of interface in MCE. In contrast, at Q_d of 8 $\times 10^{-2}$ mL h^{-1} or more, the d_{av} and CV of O/W emulsions dramatically increased to > 30 μm with CV values more than 10% (Fig. 8a). Moreover the droplet size distribution became wider and shifted towards large droplet size area. The CMS 6-2 plate used here enabled the production of O/W emulsions with uniformly sized droplets at a critical Q_d of 8 × 10^{-2} mL h^{-1}, which was higher than a maximum Q_d (5 $\times 10^{-3}$ mL h^{-1}) for the previously reported studies from grooved MCE.[42]

After reaching the critical Q_d, some of the dispersed phase that passed through the MCs expanded instead of generating droplets, suggesting that the flow state of the dispersed phase was affected by the dispersed-phase velocity inside the MC. Sugiura *et al.*[21] reported that the droplet generation behavior inside MCs are related to the capillary number of the dispersed phase that flows inside MCs. The capillary number (Ca), which indicates the balance between viscous force and interfacial force, can be determined by:

$$Ca = n_d U_d / \gamma \qquad (6)$$

where η_d is the dynamic viscosity (Pa.s) of the dispersed phase, U_d is the dispersed phase velocity inside an MC (m s^{-1}) and γ is the interfacial tension between the two phases (N m^{-1}). *Ca* at the critical Q_d of 8 × 10^{-2} mL h^{-1} was 0.017. This critical *Ca* value was similar to the previous findings with grooved MCE.[21, 43]

The influence of Q_d on the droplet generation frequency per MC array plate (*f*) (Fig. 8b) can be estimated by:

$$f = \frac{Q_d}{V_{av}} = \frac{6Q_d}{\pi d_{av}^3} \qquad (7)$$

where V_{av} is the average droplet volume. The f increased with increasing Q_d in the range of 8×10^{-2} mL h^{-1} or less. Further increase in Q_d lowered the f, and uniform fine droplets were generated at a maximum f of 8.0×10^6 h^{-1} (Fig. 8b).

Stability evaluation of ergocalciferol-loaded O/W emulsions prepared by MCE

Stability and EE of the emulsion system is directly depended on the droplet size and droplet size distribution. The more monodisperse is the system, the better the efficiency of process parameters. Grooved MCE provides useful information regarding basic characterization of droplet generation, whereas its drawback lies in low droplet productivity (e.g. a maximum of 1.5×10^{-3} L h^{-1}).[25] In comparison, straight-through MCE can increase the throughput capacity of droplets and work even at Q_d of 0.27 L h^{-1} with uniform droplet productivity.[44] Straight-through MC arrays comprised of narrow microholes and microslots that can accommodate $>10^4$ asymmetric MCs per 1 cm^2.[45] Here we focus on the stability and encapsulation efficiency of soybean oil loaded-ergocalciferol O/W emulsions prepared by straight-through MCE.

Effect of dispersed phase flux on droplet size stability during storage

Fig. 9a shows the effect of J_d on the $d_{3,2}$ and RSF of the oil droplets containing ergocalciferol prepared using WMS 11-1 plate. Dispersed phase flux (J_d) is a useful indicator of droplet productivity via MCs as well as other microfabricated devices. J_d is defined as:

$$J_d = \frac{Q_d}{A_{MCA}} \qquad (8)$$

where A_{MCA} is the total active area of the MC array (10×10 mm^2). The maximum Q_d used here was 2 mL h^{-1} which corresponds to J_d of 20 L m^{-2} h^{-1}, as it was the critical value in this study. After crossing this critical J_d there was continuous outflow of dispersed phase via some MCs, resulting in unstable droplet production. There was little increase in the $d_{3,2}$ of the resultant O/W emulsions with increasing J_d of 20 L m^{-2} h^{-1} or less (Fig. 9a). Their $d_{3,2}$ ranged between 33.9 and 35.4 μm. Their RSF

was less than 0.4 and slowly increased with increasing J_d, demonstrating monodispersity of the ergocalciferol-loaded O/W emulsions prepared here. The droplet production behavior with varying J_d was presented in Fig. 9b. There was smooth detachment of oil droplets before reaching the critical J_d.

The results presented in Fig. 9 deviate with previous findings of Vladisavljevic *et al.*[44] They reported the size stable zone of soybean oil-in-water emulsions which ranged between 0 and 50 L m^{-2} h^{-1}. Moreover, they reported critical J_d of 260 L m^{-2} h^{-1} for soybean oil loaded emulsions without loading any bioactive computed from CFD simulations. Our results are somewhat similar to the findings of Neves *et al.*[30] They formulated soybean oil-in-water emulsions loaded with polyunsaturated fatty acid at a critical J_d of 80 L m^{-2} h^{-1}. It should be noted that the flow rate of the continuous phase hardly affected the $d_{3,2}$ and RSF of the O/W emulsions encapsulating ergocalciferol (Fig. 9c), which is another advantage for stable preparation of emulsion droplets.

The monodisperse O/W emulsions loaded with ergocalciferol prepared using WMS11-1 plate were stored at 4 ± 1°C for 15 d. MCE was performed by keeping J_d at 5 L m^{-2} h^{-1} and Q_c of 150 mL h^{-1}. Immediately after collection, the O/W emulsion samples had a colorless turbid appearance with good flowability. Their appearance did not change with storage time. Fig. 10 depicts time changes in the $d_{3,2}$ and RSF values of the resultant O/W emulsions loaded with ergocalciferol. There was hardly any increase in their $d_{3,2}$ and RSF values during evaluated storage time, indicating high physical stability of the monodisperse O/W emulsions loaded with ergocalciferol.

Encapsulation efficiency of ergocalciferol in O/W emulsions

The freshly prepared O/W emulsions had an initial ergocalciferol retention of 0.06 mg mL^{-1} and regarded as 100% encapsulated efficiency (EE), since in MCE it was difficult to maintain the volume fraction with passage of time in comparison to conventional emulsification processes. Fig. 11 shows the EE and retention of ergocalciferol in the O/W emulsions prepared by MCE. The EE of ergocalciferol slightly decreased with storage time, reaching 76% after 15 d of storage at 4 °C. This

result is comparable with EE of previously encapsulated bioactives in MCE. For example, the EE of L-ascorbic acid in the W/O/W emulsions prepared through MCE was >80% after 10 d of storage.[31] These high EE values can be ascribed to very mild droplet-generation process as well as narrow droplet size distribution. It should be noted that droplet generation in MCE is based upon spontaneous transformation of the oil-water interface over the MC outlets rather than high-energy homogenization processes[46]. The EE with conventional devices like high pressure homogenizer and rotor-stator homogenizer were significantly lower (about <50%, data not shown) than MCE (>75%). The energy efficiency in MCE was around 27%, while that in conventional devices like high pressure homogenizers was very low around 0.1%.[47,48] However, scale up of MCE is still an ongoing process.

The potential reason for such decrease is the conversion of ergocalciferol to its isomeric form, isotachysterol. This conversion is accelerated in the presence of light and under slight acidic condition. In conventional emulsification system this process is highly accelerated due to heat and other stress conditions, and the EE are always lower around 60% even within one week of storage. In comparison MCE system improves the stability as well as encapsulation efficiency up to two weeks of storage. In our research these emulsions were stored at 4^{o}C and most of the emulsion samples encapsulating ergocalciferol were subjected to this optimum temperature for storage. In our previous study we found no prominent different in EE of O/W emulsions encapsulating both ergocalciferol and cholecalciferol and at 4 and 25^{o}C.[34]

Semo *et al.* [49] encapsulated ergocalciferol in casein micelles, having initial EE of over 85%. Moreover, the concentration of ergocalciferol in casein micelles was about 5.5 times than the concentration in serum surrounding around micelles. Ron *et al.*[50] encapsulated ergocalciferol in β-lg stabilized nanoparticles. The concentration of ergocalciferol in nanoparticles was 55 times higher in comparison to unbounded ergocalciferol. Ergocalciferol encapsulated in the above-mentioned studies

419 performed better against oxygen diffusion, interaction with oxidizing agents and harmful effects of
420 UV radiations. The evaluation of these mechanisms is beyond the scope of the present study.

421 ## Conclusions

422 Monodisperse food-grade O/W emulsions loaded with ergocalciferol were successfully
423 formulated through grooved MCE and straight-through MCE. The key point of our findings is stable
424 generation of uniformly sized O/W droplets that encapsulate ergocalciferol via MC arrays of
425 asymmetric microstructure, without any coalescence or wetting of dispersed phase during MCE.
426 Successful grooved MCE is achieved with different food grade ingredients as dispersed and
427 continuous phases. The high throughput studies with straight-through MCE indicates successful
428 operating conditions under a critical dispersed phase flux as well as under 1% (w/w) Tween 20 as an
429 optimum emulsifier in the continuous phase. There was hardly any increase in droplet size during 15
430 days of storage period. The resultant O/W emulsions containing ergocalciferol have encapsulating
431 efficiency of more than 75% after 15 days of storage time. The improved physical and chemical
432 stability correlate well with the monodispersity of the emulsion system. Our results indicate that
433 MCE is a promising technique for encapsulating bioactive compounds, with superior control of
434 processing parameters and various other physical conditions. The forthcoming scaling up of MCE
435 devices is expected to further improve the production capacity of emulsions, so that making it
436 practical on industrial scales through much more throughput production capacities.

437

438

439

440

441

Figures and Table captions

Figure 1: Chemical structures of important forms of vitamin D. (a) Ergocalciferol. (b) Cholecalciferol.

Figure 2: (a) Schematic drawings of the grooved MC array plate (CMS 6-2) and part of an MC array together with different dimensions. (b) Schematic drawings of the straight-through MC array plate (WMS 11-1) and MCs dimensions.

Figure 3: (a) Schematic drawing of a grooved MCE setup. (b) Schematic drawing of droplet generation via part of an MC array having 5 μm depth.

Figure 4: (a) Schematic representation of a straight-through MCE setup. (b) Droplet generation representation through asymmetric MCs.

Figure 5: (a) Effect of different dispersed phase composition on d_{av} and CV of O/W emulsions. (▭) denotes d_{av} of different dispersed phases, while (●) denotes CV of different dispersed phases. (b) Typical generation behaviors of O/W emulsions droplets encapsulating ergocalciferol by using different dispersed phase oils. (c) Micrographic images of droplets encapsulating ergocalciferol using different dispersed phases.

Figure 6: Effect of different emulsifiers on droplet generation behavior in grooved MCE. (a) Droplet generation with (*i*) Tween 20, (*ii*) Sunsoft A-12 and (*iii*) β-lg. (b) Effect of different emulsifiers on d_{av} and CV of O/W emulsions, (▭) denotes d_{av} of different emulsifiers, while (●) denotes CV of different emulsifiers. (c) Typical droplet generation characteristics with β-lg as emulsifier.

Figure 7: Effect of ergocalciferol concentration in soybean oil on d_{av} and CV of O/W emulsions either stabilized by 1% (w/w) Tween 20 or Sunsoft A-12.

Figure 8: (a) Effect of Q_d on d_{av} and CV of the O/W emulsions encapsulating soybean oil loaded-ergocalciferol produced using the CMS 6-2 plate. (b) Effect of Q_d on the droplet generation frequency per hour.

Figure 9: (a) Effect of dispersed phase flux (J_d) on sauter mean diameter ($d_{3,2}$) and relative span factor (RSF) of O/W emulsions encapsulating ergocaliferol. (b) Typical droplet generation behavior at (i) low flux of 5 L m^{-2} h^{-1} and (ii) critical flux of 20 L m^{-2} h^{-1}. (c) Effect of continuous phase flow rate (Q_c) on $d_{3,2}$ and RSF of O/W emulsions encapsulating ergocalciferol.

Figure 10: Storage stability of O/W emulsions encapsulating ergocalcifierol stored at 4 ±1^{o}C. The data was presented in term of $d_{3,2}$ and RSF.

Figure 11: Encapsulating efficiency and retention profile of O/W emulsions with storage time. The emulsions were prepared at J_d of 5 L m^{-2} h^{-1}, and the data was presented over 15 days of storage time.

Table 1: Fluid properties of the systems containing ergocalciferol together with different oils used for preparing O/W emulsions

References

1. M. T. Cantorna and B. D. Mahon, *Exp. Biol. Med.*, 2004, **229**, 1136-1142.
2. E. Hypponen, E. Laara, A. Reunanen, M. R. Jarvelin and S. M. Virtanen, *Lancet*, 2001, **358**, 1500-1503.
3. J. Kendrick, G. Targher, G. Smits and M. Chonchol, *Atherosclerosis*, 2009, **205**, 255-260.
4. J. M. Lappe, D. Travers-Gustafson, K. M. Davies, R. R. Recker and R. P. Heaney, *Am. J. Clin. Nutr.*, 2007, **85**, 1586-1591.
5. F. Bandeira, A. G. Costa, M. A. Soares Filho, L. Pimentel, L. Lima and J. P. Bilezikian, *Arq. Bras. Endocrinol. Metabol.*, 2014, **58**, 504-513.
6. I. G. Song and C. J. Park, *Blood Res.*, 2014, **49**, 84.
7. L. M. Ward, I. Gaboury, M. Ladhani and S. Zlotkin, *Can. Med. Assoc. J.,* 2007, **177**, 161-166.
8. R. W. Chesney, *Pediatr. Int.*, 2003, **45**, 509-511.
9. M. F. Holick, *J. Cell. Biochem.*, 2003, **88**, 296-307.
10. M. F. Holick, *J. Investigative Med.*, 2011, **59**, 872-880.
11. R. B. Japelt and J. Jakobsen, *Front. Plant Sci.*, 2013, **4**, 136.
12. T. D. Thacher and B. L. Clarke, *Mayo Clin. Proc.*, 2011, **86**, 50-60.
13. L. A. Armas, B. W. Hollis and R. P. Heaney, *J. Clin. Endocrinol. Metabol.*, 2004, **89**, 5387-5391.
14. H. M. Trang, D. E. Cole, L. A. Rubin, A. Pierratos, S. Siu and R. Vieth, *Am. J. Clin. Nutr.*, 1998, **68**, 854-858.
15. L. A. Houghton and R. Vieth, *Am. J. Clin. Nutr.*, 2006, **84**, 694-697.
16. R. R. Eitenmiller, W. Landen Jr and L. Ye, *Vitamin analysis for the health and food sciences*, CRC Press, 2007.
17. M. R. Patel and M. F. San Martin-Gonzalez, *J. Food Sci.*, 2012, **77**, N8-N13.

18. L. L. Schramm, *Microscience and Applications of Emulsions, Foams, Suspensions, and Aerosols*, John Wiley & Sons, 2014.

19. D. J. McClements, *Crit. Rev. Food Sci. Nutr.*, 2007, **47**, 611-649.

20. G. T. Vladisavljevic, N. Khalid, M. A. Neves, T. Kuroiwa, M. Nakajima, K. Uemura, S. Ichikawa and I. Kobayashi, *Adv. Drug Deliv. Rev.*, 2013, **65**, 1626-1663.

21. S. Sugiura, M. Nakajima, N. Kumazawa, S. Iwamoto and M. Seki, *J. Physical Chem. B.*, 2002, **106**, 9405-9409.

22. G. T. Vladisavljevic', I. Kobayashi and M. Nakajima, *Microfluid Nanofluid.*, 2012, **13**, 151-178.

23. I. Kobayashi, S. Mukataka and M. Nakajima, *Ind. Eng. Chem. Res.*, 2005, **44**, 5852-5856.

24. I. Kobayashi, Y. Wada, Y. Hori, M. A. Neves, K. Uemura and M. Nakajima, *Chem. Eng. Technol.*, 2012, **35**, 1865-1871.

25. I. Kobayashi, Y. Wada, K. Uemura and M. Nakajima, *Microfluid Nanofluid.*, 2010, **8**, 255-262.

26. S. Sugiura, M. Nakajima, J. H. Tong, H. Nabetani and M. Seki, *J. Colloid Interface Sci.*, 2000, **227**, 95-103.

27. F. Ikkai, S. Iwamoto, E. Adachi and M. Nakajima, *Colloid Polymer Sci.*, 2005, **283**, 1149-1153.

28. S. Sugiura, T. Kuroiwa, T. Kagota, M. Nakajima, S. Sato, S. Mukataka, P. Walde and S. Ichikawa, *Langmuir.*, 2008, **24**, 4581-4588.

29. M. A. Neves, H. S. Ribeiro, I. Kobayashi and M. Nakajima, *Food Biophys.*, 2008, **3**, 126-131.

30. M. A. Neves, H. S. Ribeiro, K. B. Fujiu, I. Kobayashi and M. Nakajima, *Ind. Eng. Chem. Res.*, 2008, **47**, 6405-6411.

31. N. Khalid, I. Kobayashi, M. A. Neves, K. Uemura, M. Nakajima and H. Nabetani, *Colloid Surface A.*, 2014, **458**, 69-77.

32. N. Khalid, I. Kobayashi, M. A. Neves, K. Uemura, M. Nakajima and H. Nabetani, *Colloid Surface A.,* 2014, **459**, 247-253.

33. S. Souilem, I. Kobayashi, M. Neves, S. Sayadi, S. Ichikawa and M. Nakajima, *Food Bioprocess Technol.*, 2014, **7**, 2014-2027.

34. N. Khalid, I. Kobayashi, Z. Wang, M. A. Neves, K. Uemura, M. Nakajima and H. Nabetani, *Int. J. Food Sci. Technol.*, 2015, **50**, 1807-1814.

35. Z. Wang, M. A. Neves, I. Kobayashi and M. Nakajima, *Controlling properties of micro-to nano-sized dispersions using emulsification devices*, Wiley-Blackwell, Oxford, UK, 2015.

36. O. Brand, G. K. Fedder, C. Hierold, J. G. Korvink, O. Tabata and N. Kockmann, *Micro process engineering: fundamentals, devices, fabrication, and applications*, John Wiley & Sons, 2013.

37. I. Kobayashi, S. Mukataka and M. Nakajima, *J. Colloid Interface Sci.*, 2004, **279**, 277-280.

38. K. van Dijke, I. Kobayashi, K. Schroen, K. Uemura, M. Nakajima and R. Boom, *Microfluid Nanofluid.*, 2010, **9**, 77-85.

39. C. Tan, I. Kobayashi and M. Nakajima, *Preparation of monodispersed refined-bleached-deodorized (RBO) palm olein-in-water emulsions by microchannel emulsification.* Proceedings of the International Chemical Congress of Pacific Basin Societies, December 15-20, 2005. Honolulu, Hawaii.

40. I. Kobayashi and M. Nakajima, *Eur. J. Lipid Sci. Technol.*, 2002, **104**, 720-727.

41. N. Khalid, I. Kobayashi, M. A. Neves, K. Uemura, M. Nakajima and H. Nabetani, *Biosci. Biotechnol. Biochem.*, 2015, DOI: 10.1080/09168451.2015.1050988.

42. T. Kawakatsu, G. Tragardh, Y. Kikuchi, M. Nakajima, H. Komori and T. Yonemoto, *J. Surfactants Deterg.*, 2000, **3**, 295-302.

43. I. Kobayashi, M. A. Neves, Y. Wada, K. Uemura and M. Nakajima, *Procedia Food Sci.*, 2011, **1**, 109-115.

44. G. T. Vladisavljevic, I. Kobayashi and M. Nakajima, *Microfluid Nanofluid.*, 2011, **10**, 1199-1209.

45. I. Kobayashi, S. Mukataka and M. Nakajima, *Langmuir.*, 2005, **21**, 7629-7632.

46. S. Sugiura, M. Nakajima, S. Iwamoto and M. Seki, *Langmuir.*, 2001, **17**, 5562-5566.

47. I. Kobayashi, T. Takano, R. Maeda, Y. Wada, K. Uemura and M. Nakajima, M, *Microfluid Nanofluid*., 2008, **4**, 167-177.

48. S. Schultz, G. Wagner, K. Urban and J. Ulrich, *Chem. Eng. Technol*., 2004, 27, 361-368.

49. E. Semo, E. Kesselman, D. Danino and Y. D. Livney, *Food Hydrocoll.*, 2007, **21**, 936-942.

50. N. Ron, P. Zimet, J. Bargarum and Y. D. Livney, *Int. Dairy J.*, 2010, **20**, 686-693.

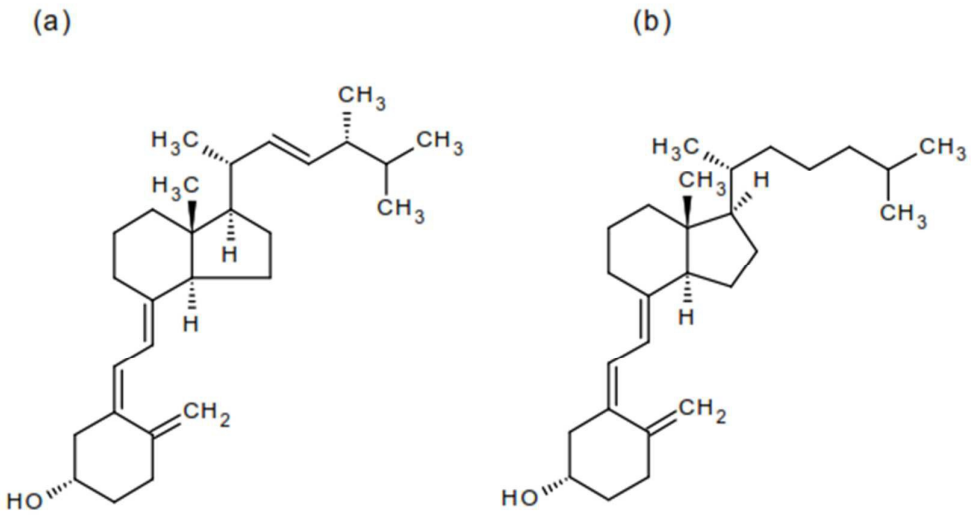

Figure 1

(a)

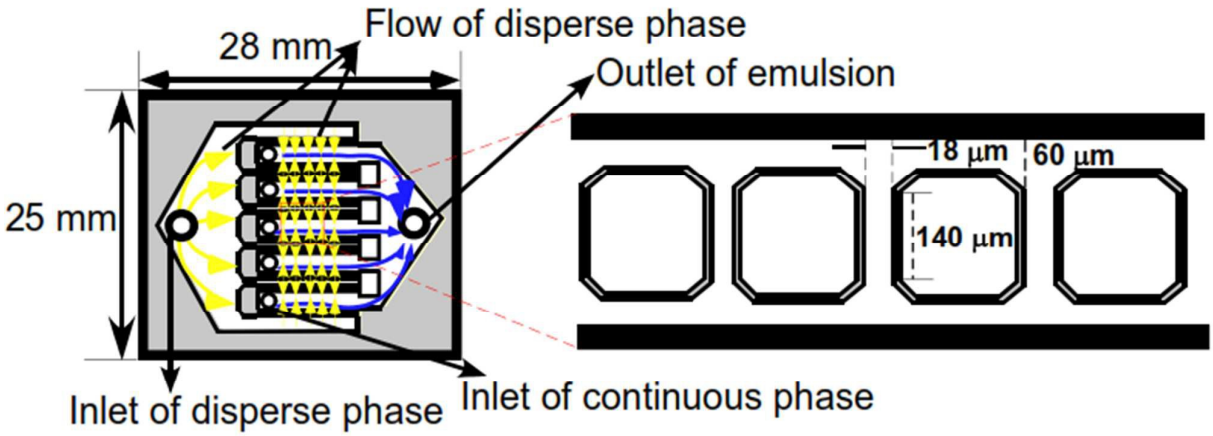

(b)

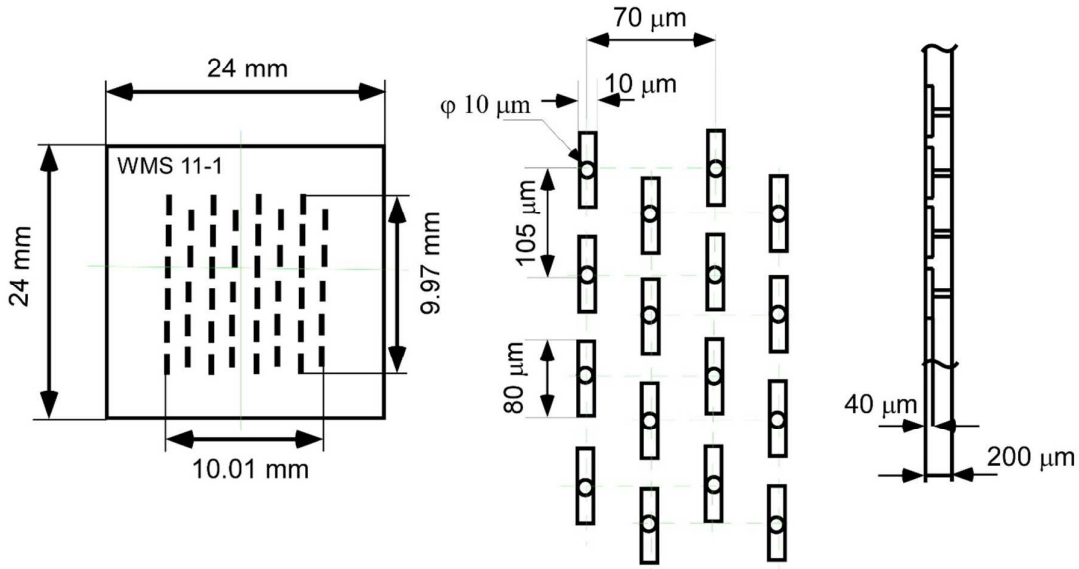

Figure 2

24

25

26 **(a)**

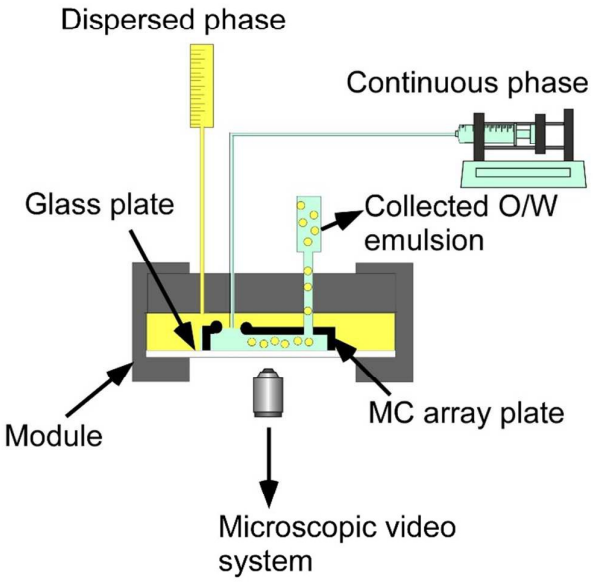

27

28 **(b)**

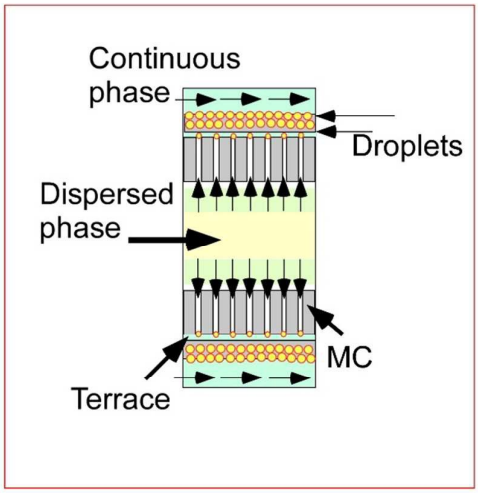

29

30 **Figure 3**

(a)

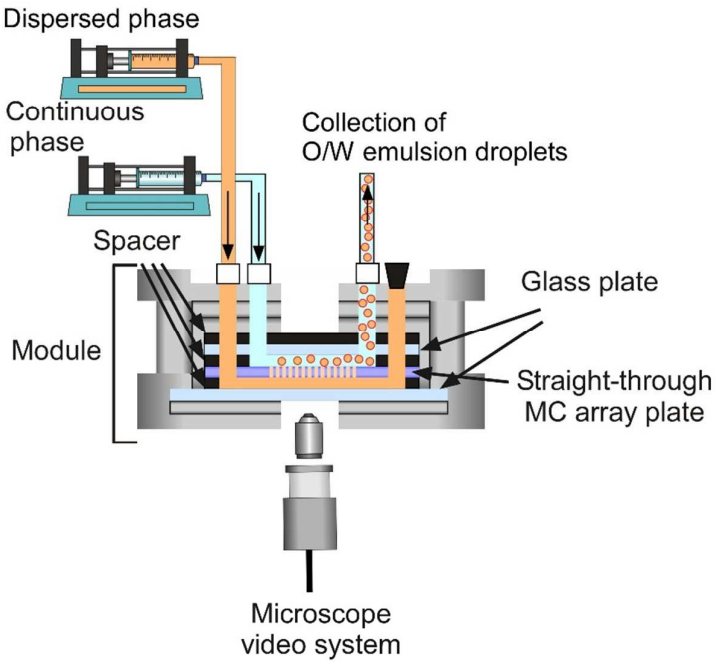

(b)

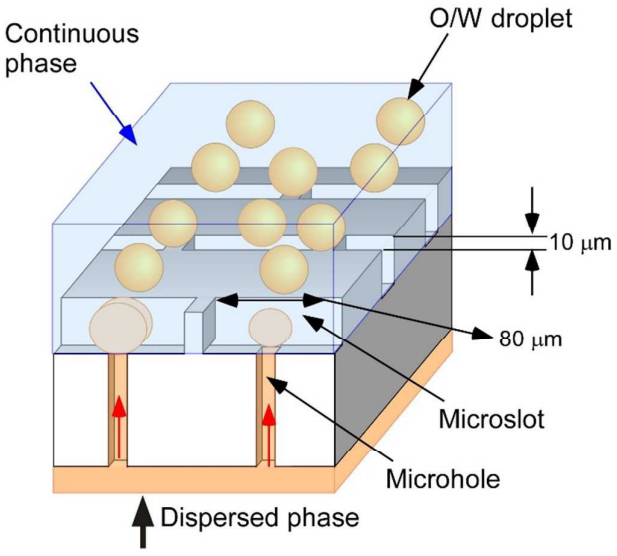

Figure 4

(a)

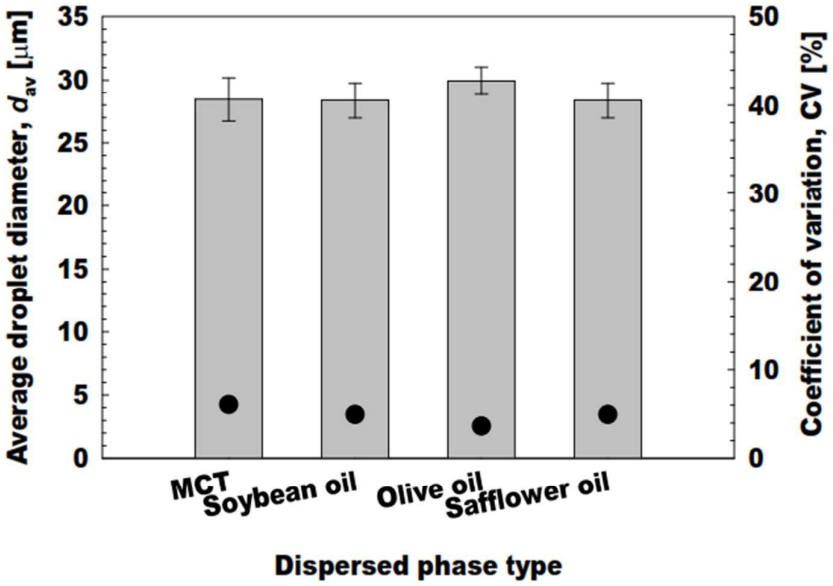

(b)

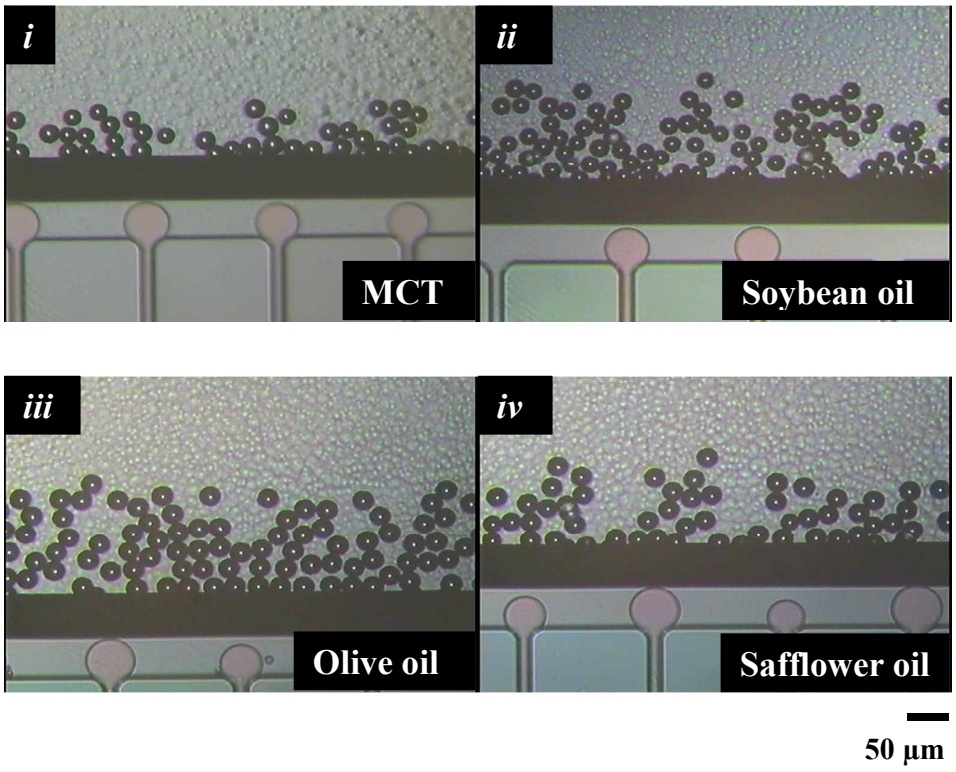

Figure 5

(c)

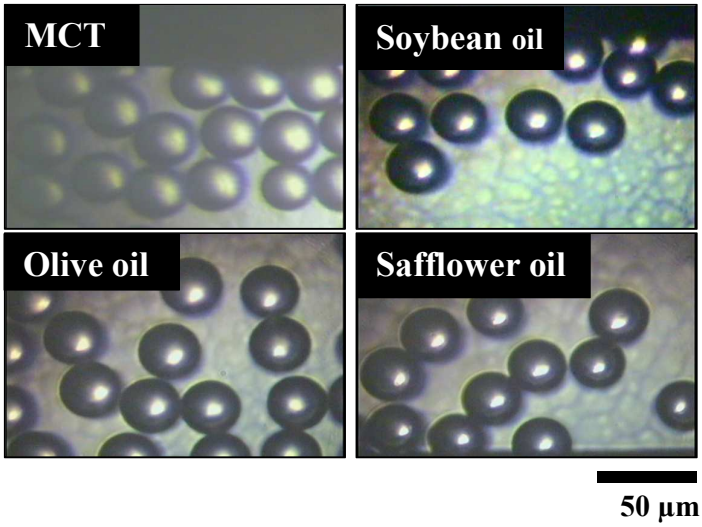

Figure 5 (cont.)

(a)

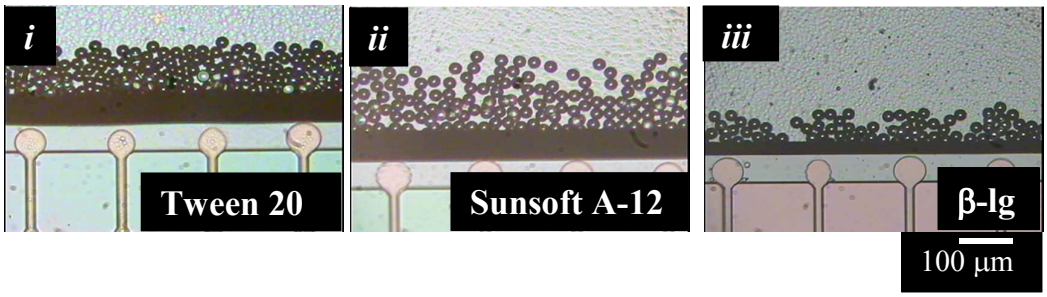

(b)

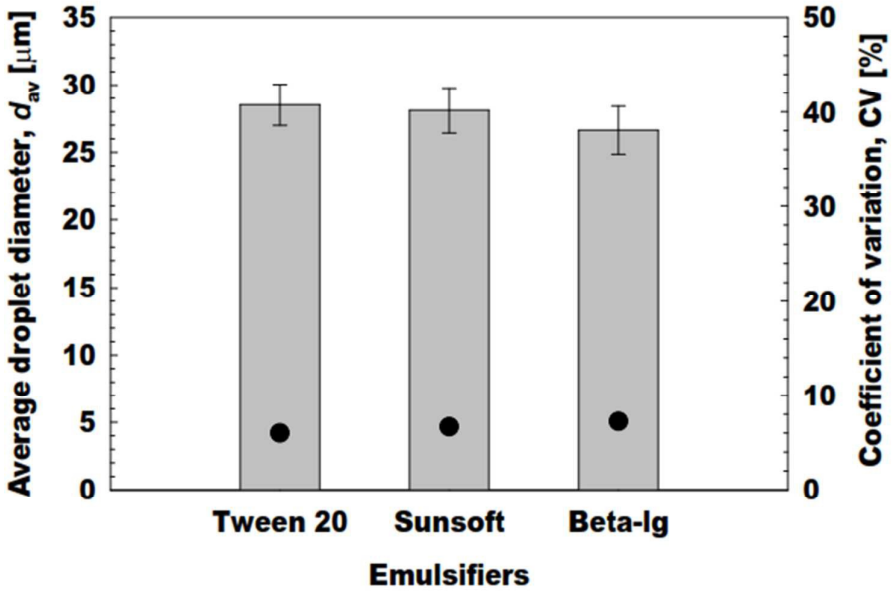

(c)

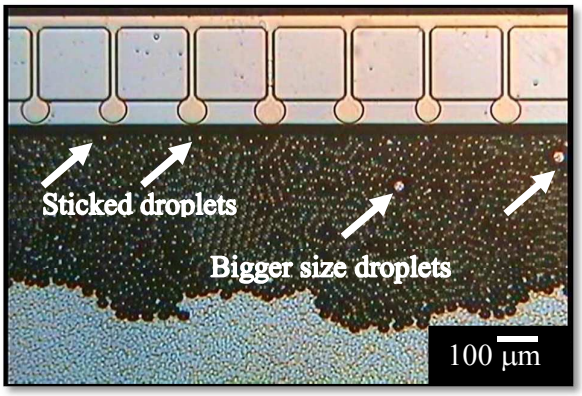

Figure 6

72

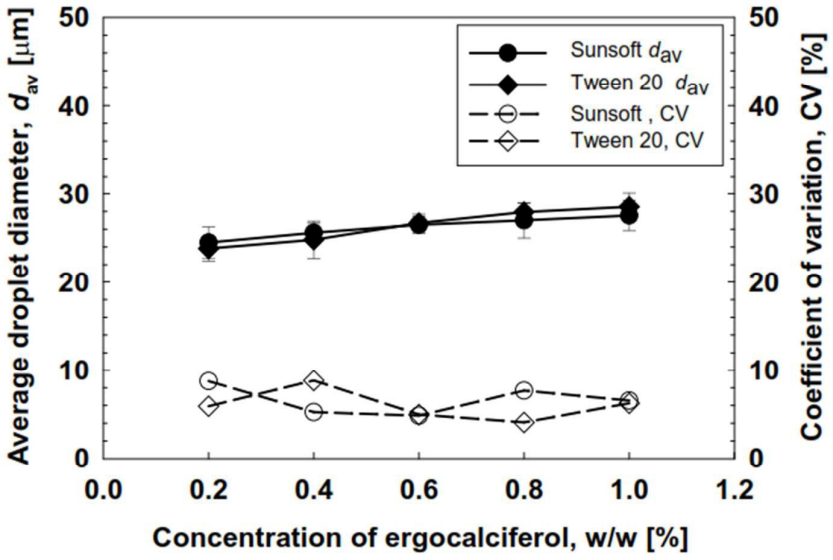

73

74 **Figure 7**

75

(a)

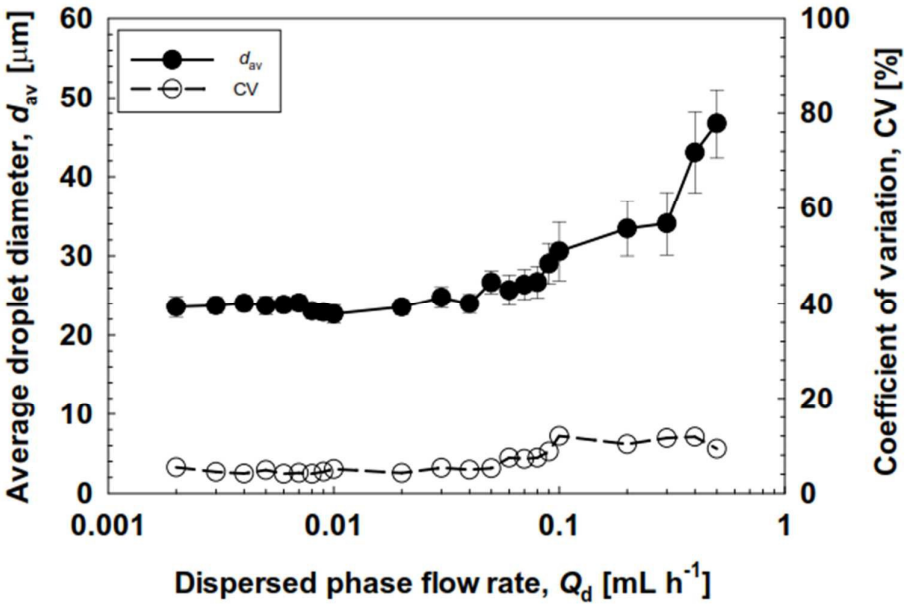

(b)

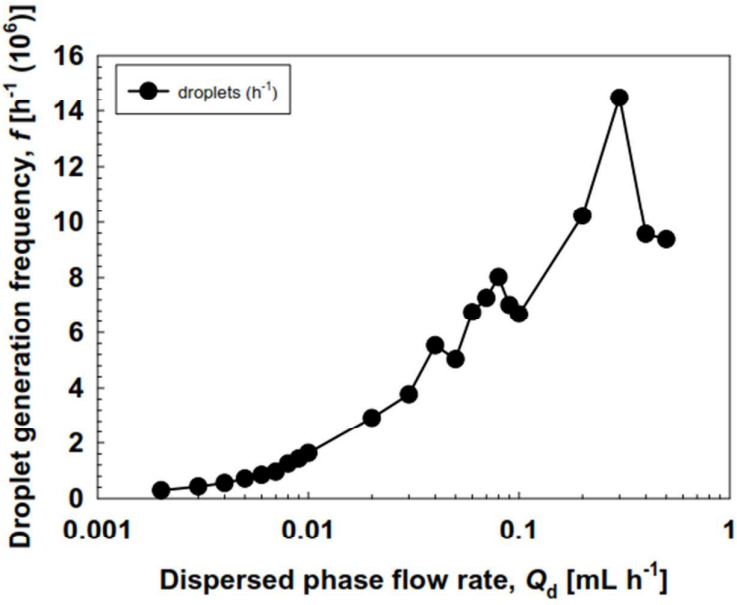

Figure 8

82 **(a)**

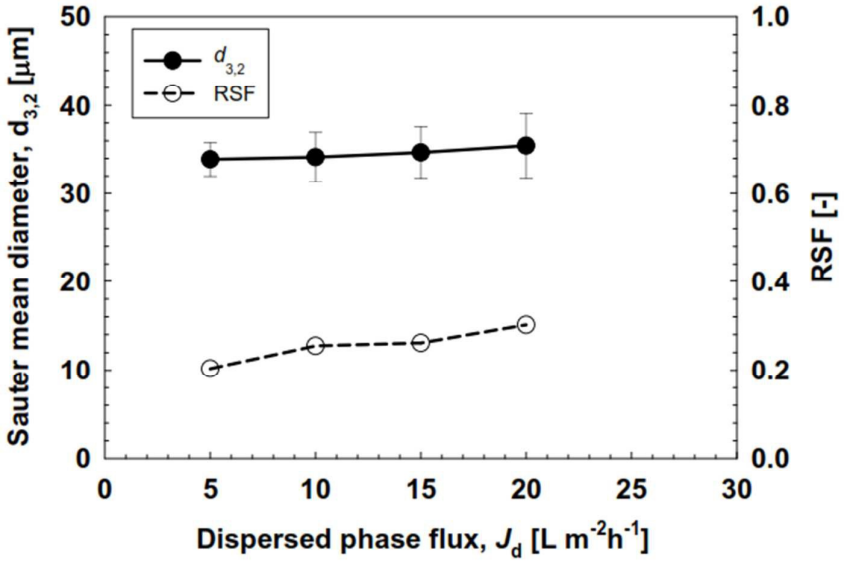

83

84

85 **(b)**

86

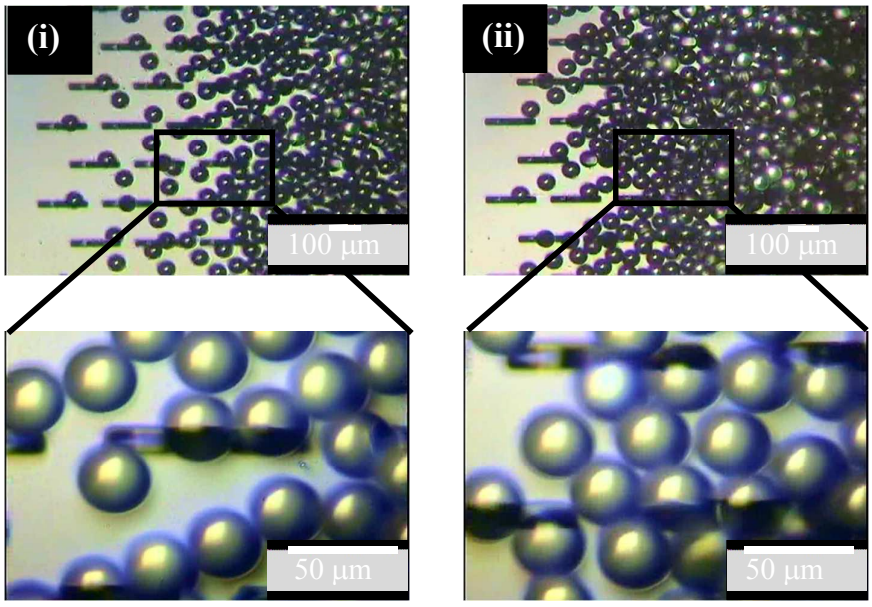

87

88

89

90

(c)

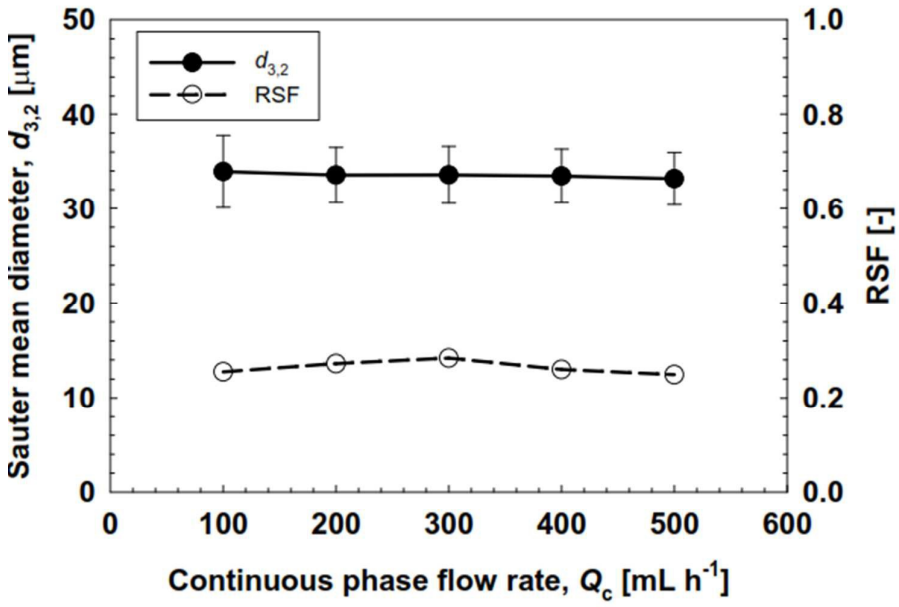

Figure 9

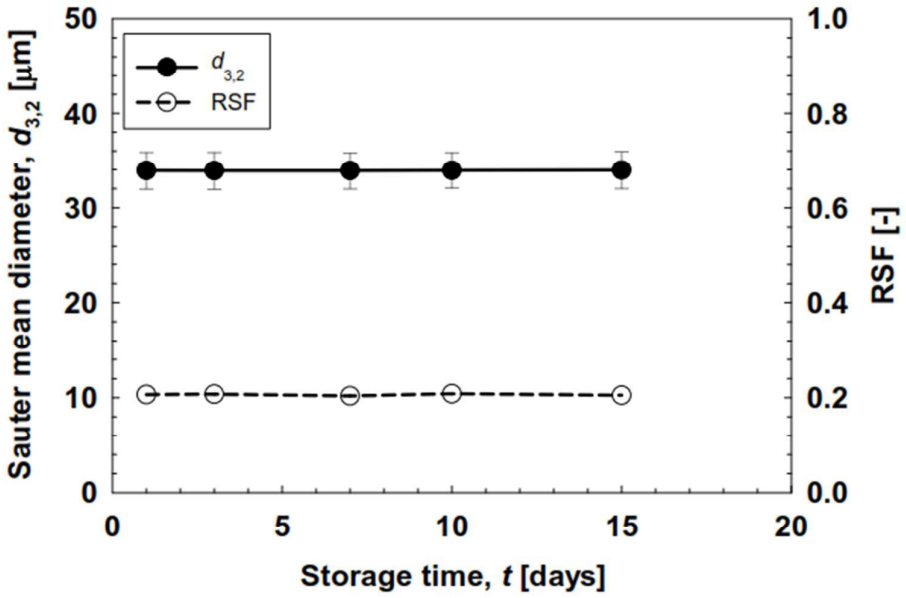

100

101 **Figure 10**

102

103

104

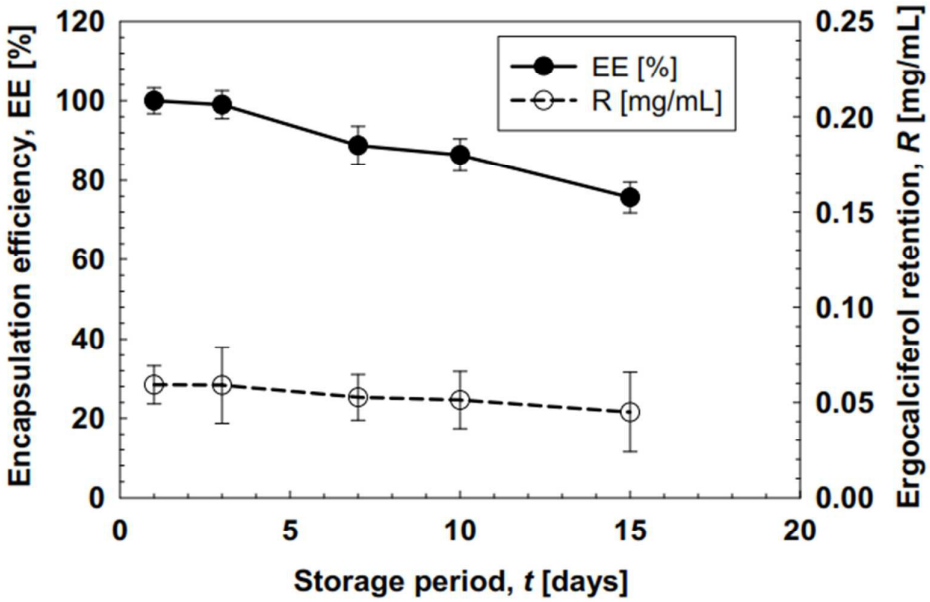

105

106 **Figure 11**

107

108

109

110

111

112

113

114

115

116

Table 1: Fluid properties of the systems containing ergocalciferol together with different oils used for preparing O/W emulsions

	Dispersed phase				Continuous phase			
	η_d (mPa s)	ρ_d (kg m^{-3})	γ_d (mN m^{-1})	**ζ (–)	Emulsifiers in Milli-Q water	η_c (mPa s)	ρ_c (kg m^{-3})	γ_c (mN m^{-1})
***MCT**	22.5±0.3	946.9±0.2	5.3±0.4	24.7	0.5% Tween 20	0.89±0.1	997.3±0.6	5.1±0.2
***Soybean oil**	53.0±0.1	921.9±0.4	5.6±0.1	58.2	1.0% Tween 20	0.91±0.1	998.4±0.6	5.2±0.1
***Olive oil**	68.2±0.1	911.9±0.2	6.2±0.2	75.0	1.5% Tween 20	0.96±0.1	999.1±0.8	5.2±0.2
***Safflower oil**	53.2±0.1	918.9±0.1	5.3±0.2	58.5	2.0% Tween 20	0.99±0.1	1000.1±0.1	5.4±0.3
					1.0% β-lg	0.95±0.1	999.9±0.2	12.6±0.9
					1.0% Sunsoft A-12	0.97±0.1	998.5±0.6	4.8±0.2

* Dispersed phase contains 0.5% (w/w) ergocalciferol and interfacial tension was measured in the presence of 1% (w/w) Tween 20 in Milli-Q water, ** Viscosity ratio (ζ) was defined as the ratio of dispersed phase viscosity over continuous phase viscosity